

UNIVERSITE PARIS-SACLAY
Teaching Centre: Université d'Evry Val d'Essone

NETLOGO PROJECT: EPITHELIOMHE IMPLEMENTATION

Student: Janio Paternina
M2 GENIOMHE
2015-2016

TABLE OF CONTENTS

Contents

Epitheliome: the model	1
The extracellular medium and external parameters	1
Cells are modelled as turtles	1
Cell cycle dynamics	1
Cell bonding	3
Cell migration	3
Cellular sub-types	3
Model simulations	5
Cell growth dynamics	5
1. Urothelial cells	5
2. Keranocytes	7
Wound healing	8
1. Urothelial cells	8
2. Keranocytes	10
Conclusions	13
References	14

Epitheliome: the model

The present report introduces a NetLogo—Wilensky, U. (1999)—implementation of the Epitheliome, an agent-based model which mimics a single-layer epithelial tissue, based on the rules and simulations carried out by Walker et al. (2004, 2004). In their study, they defined simple growth, migration, and bonding rules in order to analyse the social behaviour of cells at the population level, and how this behaviour varies according to parameters such as cellular type, extracellular calcium, and tissue wounding.

THE EXTRACELLULAR MEDIUM AND EXTERNAL PARAMETERS

The extracellular medium of this model consists of a bidimensional *world* with dimensions of 60 x 60 patches. In order to simulate several world sizes without modifying the world size directly, the parameter *scale* was introduced; this variable scales the cells dimensions such that, if its value is set to 20, each unit observed in the world corresponds to 20 μm .

In the present model, patches are only handled to visualise, with a colour code, the two calcium concentrations that were taking into account in the study: low (0.09 mM) and physiological (2.0 mM). It is possible, as well, to simulate cell cultures of both keranocytes and urothelial cells, which have cell cycle length differences.

Finally, it is also possible to vary the initial seeded cell number from 10 to 100.

CELLS ARE MODELLED AS TURTLES

Epithelial cells are implemented as NetLogo turtles, due to their capability of migration. Thus, each cell is modelled as a circular shaped turtle, whose size depends on two variables: the *true* radius, and the *apparent* or *spread* radius (*s-radius*), which corresponds to the radius that is observed from above when a cell spreads on the substrate; each cell has a volume as well, calculated from the true radius.

The remaining cell variables determine the evolution of the cell cycle and growth (including an internal counter), as well as migration distances.

CELL CYCLE DYNAMICS

Cells follow the cell cycle rules described in Walker et al. (2004), as illustrated in Table 1. Cycle length is calculated according to the cellular type, i.e. 120 iterations (60 hours) for keranocytes and 30 iterations (15 hours) for urothelial cells. The aforementioned length is considered as the mean of a normal distribution, with a variance equal to 0.1 times the mean. According to the authors of

the epitheliome, G1 stage of the cell cycle is considered to be 50% of the total cycle length. For this reason, total cell cycle length is calculated based on G1 stage length, which is in turn calculated using the `random-normal` command in NetLogo, taking base-line cycle length divided by two (60 for keranocytes, 15 for urothelial cells) as the mean, and 0.05 times the mean as the variance of the distribution. Total cycle length is then calculated by doubling G1 stage length; the whole calculation was implemented using a procedure, this in order to avoid code duplication. These values are useful to perform a follow-up of the cell cycle progression by being compared to the cell's internal counter.

Table 1. Courtesy from Walker et al. / *BioSystems* 76 (2004) 89–100.

Table 1
Summary of model rules relating to cell cycle progression

Current state		Action
Cell is in G1		Increase cell volume by set amount Increment internal counter by +1
Cell is at G1/G0 checkpoint	If cell is bonded to four or more neighbours	Enter G0
	If cell is not sufficiently spread (radius $< 1.5 \times$ 'rounded' radius)	
	Else	
Cell is in G0	If cell is bonded to less than four neighbours	Re-enter G1
	If cell sufficiently spread	
	Else	
Cell is in S/G2		Increment internal counter by +1
Cell is at G2/M boundary		Change to mitotic cell type
Cell is at end of M phase		Divide to create two identical daughter cells

With the implementation of cell sub-types and maximum number of cell divisions, an additional rule is added to the G0 or quiescent state: when in G0, a transition amplifying cell can re-enter G1 only if it has not reached its maximum number of divisions.

When a cell is in the mitotic state, it returns to a spherical shape, thus its *apparent* radius equals its true radius, and it is no longer allowed to spread or form bonds. By the end of mitosis, a given cell *divides* to produce two daughter cells. This is implemented in the model by using the `hatch-<breeds>` command. This command would create one transit amplifying daughter cell regardless of the mother's subtype. The internal counter of both daughter cells, and maximum division number are reset (the latter in order to avoid a daughter cell to inherit an indefinite number of divisions from a stem cell). Moreover, before the hatching, the volume of daughter cells is set as half the volume of the mother cell, and radius is updated accordingly. Finally, a new cell cycle length is calculated for each cell by calling the cycle calculation procedure. The newly hatched cell acquires a new direction so as to migrate differently from the other daughter cell.

CELL BONDING

In the present model, intercellular bonds are represented as links, since they are the easiest way to establish a physical relationship between turtles. Cell bonding occurs when two cells are within less than 10 μm . In order to implement this, and since NetLogo does not take into account the size when computing the distances that exist between each pair of turtles, it was necessary to use the apparent radiuses of the turtles.

Furthermore, in order to model the calcium dependence of intercellular bonding, the probability of a pair of cells to establish a cellular bond was calculated based on the experimental data collected by Baumgartner et al. (2000). This strategy effectively established bonds between nearby cells. However, it was not possible to model the bonds that are established between a given cell which is by the edge of the world and the edge itself. As a consequence, in the present model, a cell by the edge behaves as an unbounded cell.

Cells are also bounded to the substrate. This was modelled by implementing the Boolean variable `bonded?` which determines whether a cell is bound to the substrate or not. This variable is useful to cause apoptosis of unbound cells that have reached a certain point of the cell cycle. However, the probability of binding to the substrate was biased to allow a high number of cells to be bound.

CELL MIGRATION

Cells which are bound to the substrate, but which have no intercellular bonds, are capable of lateral migration. The rules were implemented as described by Walker et al. (2004).

It is important to note that physical correction was also implemented to avoid overlapping of cells. Nevertheless, after a given number of iterations, when the number of cells is high enough, migration and physical correction are in conflict, causing unnatural behaviours such as cells that *skip* over a group of other cells, or inevitably overlapping each other.

Physical correction was especially difficult to implement due to the lack of a communication matrix which informs each cell about the position of the other cells. Instead, a series of imbricated `ask other-turtles` commands were used.

CELLULAR SUB-TYPES

In the model, two cellular sub-types exist: transit amplifying cells, and stem cells. The major difference between the two is the maximum number of divisions, which is unlimited for stem cells, and of 3 or 30 for transit amplifying cells (depending on the cellular type—keranocytes and urothelial cells respectively). These sub-cellular sub-types were implanted by the use of *breeds* in NetLogo. This would not only allow the setting of the variable of maximum divisions according to

the breed, but also the implementation of different cell cycle behaviours, namely the progression from the G0 state. A colour code was used to visually distinguish cellular sub-types, using green for transit amplifying cells, pink for stem cells, and blue for transit amplifying cells that originated from stem cells.

Model simulations

Simulations were carried out by varying two main parameters: cell type (keranocytes vs. urothelial cells) and extracellular calcium concentration (low vs. physiological). The evolution over time of the number of intercellular bonds, the number of cells in the G0 state, and the total number of cells was registered by using the plots provided by NetLogo. All simulations were performed using a scale of 1:30, and generally 50 urothelial cells, and 100 keranocytes were seeded at $t = 0$.

CELL GROWTH DYNAMICS

Cellular growth was studied until cells reached confluence; in other words, until cells covered the entire world.

1. Urothelial cells

For the number of initial seeds and this cellular type, confluence was reached soon after a few number of divisions (at around 70 to 75 hours – 140 to 150 iterations), and thus no steady state was observed.

a. Low calcium concentration

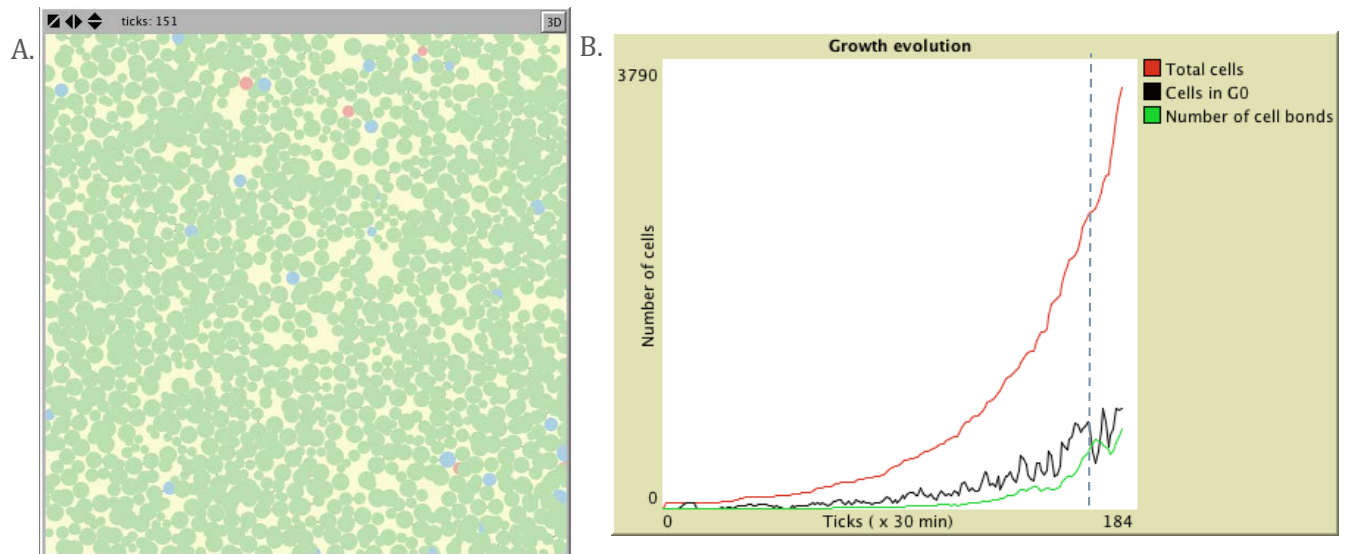


Figure 1. A. Cells after 75 hours (151 iterations). In green, TA-cells; in red, stem cells; in blue, TA-cells spawned by stem cells. B. Growth evolution of urothelial cells.

As observed in Figure 1B, the total number of cells show an exponential growth tendency. As the number of cells increases, so does the number of total intercellular bonds, although it remains significantly lower; this may be due to the increased

probability of establishing intercellular bonds when cells are forced to be close to one another.

Interestingly, the peaks of number of cells in the G0 state coincide with stabilization of cell growth, e.g. the peak pointed out by the dashed line, suggesting that a high fraction of cells in G0 slows down population growth rate.

b. High calcium concentration

Although cell growth showed similar population dynamics in high calcium concentrations to what was observed in low concentrations, the patterns that were observed before confluence were interesting (Figure 2).

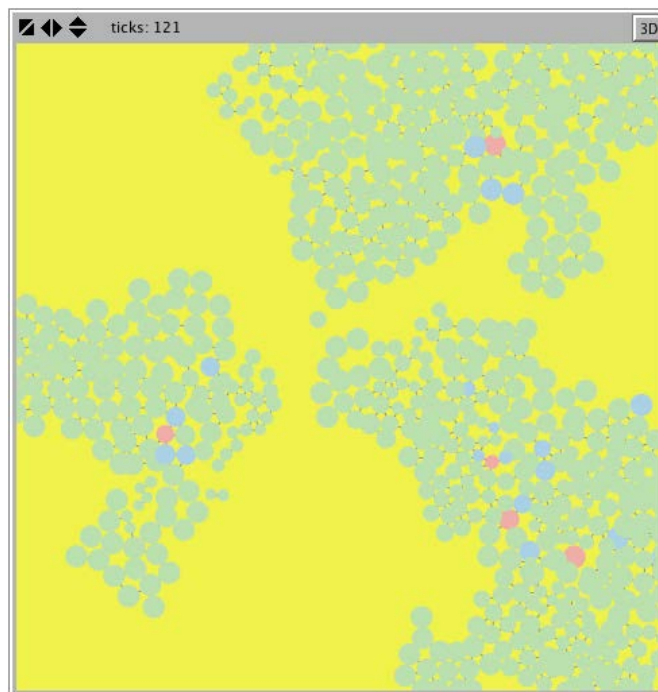


Figure 2. Cellular growth pattern observed in high extracellular calcium concentration.

Once extracellular calcium concentration increased, and thus higher probabilities of establishing intercellular bonds were obtained, cells had less migration liberty, and thus their cell cycle was carried out within what seem *colonies*. Confluence was reached when these colonies grew and fused together.

Another major difference of growth evolution was observed concerning the number of total intercellular bonds. In the presence of high calcium concentrations, the number of intercellular bonds quickly surpasses the total number of cells,

which is opposite to which was observed in low calcium concentrations (data not shown).

Finally, it is important to note that the number of TA-cells spawned by stem cells remained insignificant when compared to the total number of cells, both in low and high calcium concentrations.

2. Keranocytes

Due to longer cell cycle lengths, and a growth rate slowed down by a limited maximum number of divisions, initial seeds of keranocytes were increased from 50 to 100.

The cell growth evolution was quite similar in both calcium concentrations, showing an exponential growth at early iterations, and the reaching a steady state in which population growth rate is minimal and the number of cells in G0 state approaches the total number of cells (data not shown). Extracellular calcium concentration, however, seems to have an impact on the time necessary to reach confluence, being of around 300 hours (600 iterations) for the low calcium concentration, and of 400 hours (800 iterations) for the high calcium concentration, and in the latter case, confluence is not even complete (Figure 3). This suggests that cellular motility might be a necessary factor for rapid cellular growth.

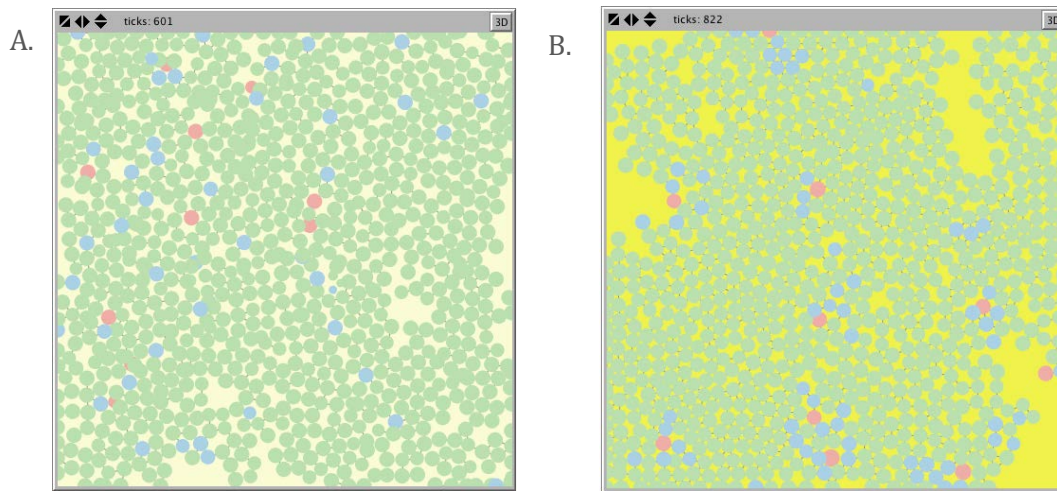


Figure 3. A. Confluence of keranocytes at low extracellular calcium concentrations (601 iterations). B. (Incomplete) confluence of keranocytes at high calcium concentrations (822 iterations).

WOUND HEALING

A procedure that *kills* all cells within 10 units of the centre of the world was implemented in order to simulate tissue wounding. The actual size of the wound obviously depends on the scale that was used. In the simulations that were carried out, with a 1:30 scale, the wound was 600 μm wide. Both growth evolution and images of the cells were studied at several points of time after the wound.

1. Urothelial cells

Rapid cellular growth made it possible to study the urothelial cells at intervals of 6 iterations (3 hours).

a. Low calcium concentration

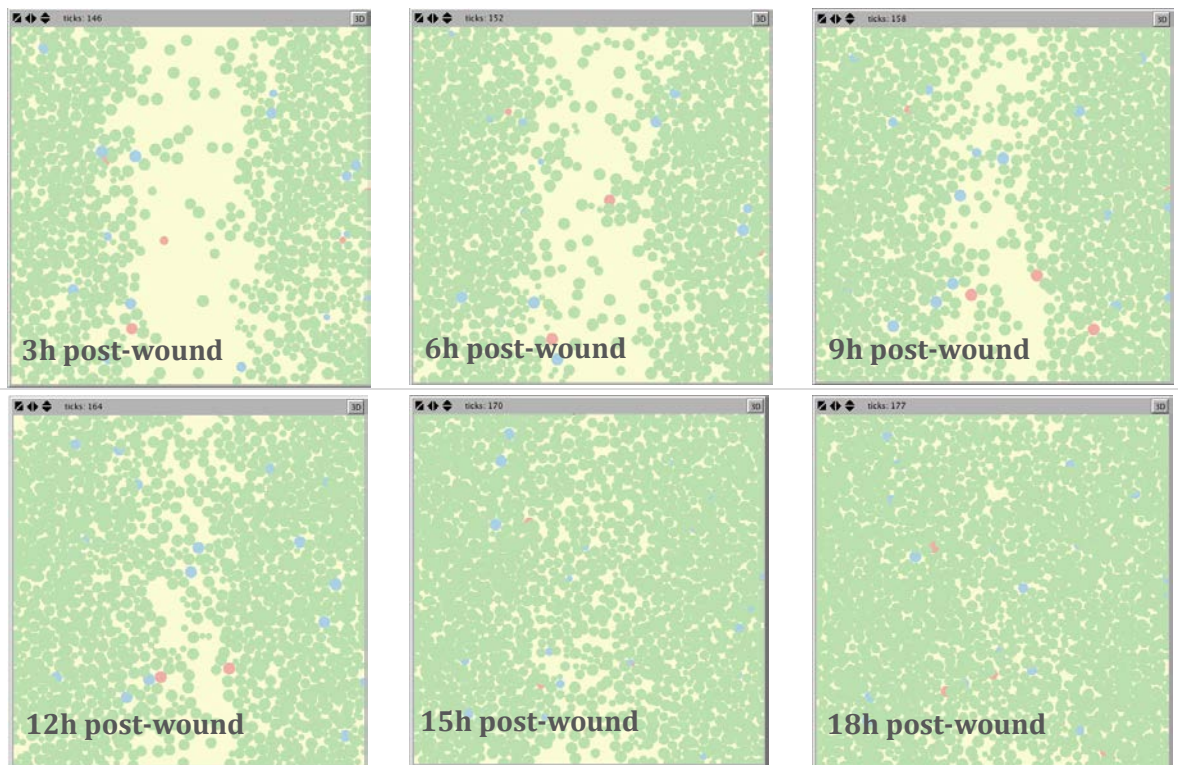


Figure 4. Wound- healing follow-up at three-hour intervals for urothelial cells at low calcium concentrations.

As seen in Figure 4, urothelial cells cover completely the wound after 18 hours. When analysing the population growth dynamics (Figure 5A), it is observed that after wounding, cell growth rate continues to be exponential and quickly surpasses the number of total cells present at the moment of wounding. When analysing the presence of cells in the wound space (Figure 5B), it is observed that the number of cells in this location is not only fully restored, but even increased after 18 hours.

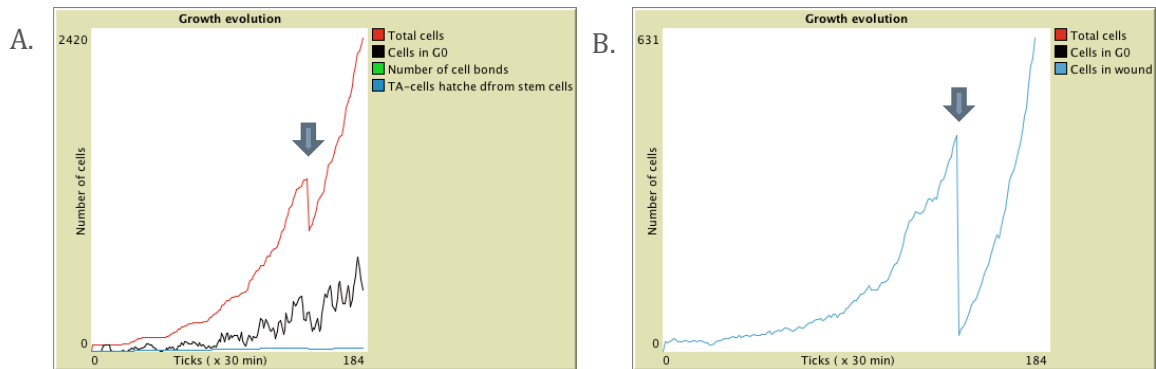


Figure 5. A. Growth evolution of urothelial cells after wound (indicated with arrow). B. Evolution of number of cells occupying the space of the wound.

b. High calcium concentration

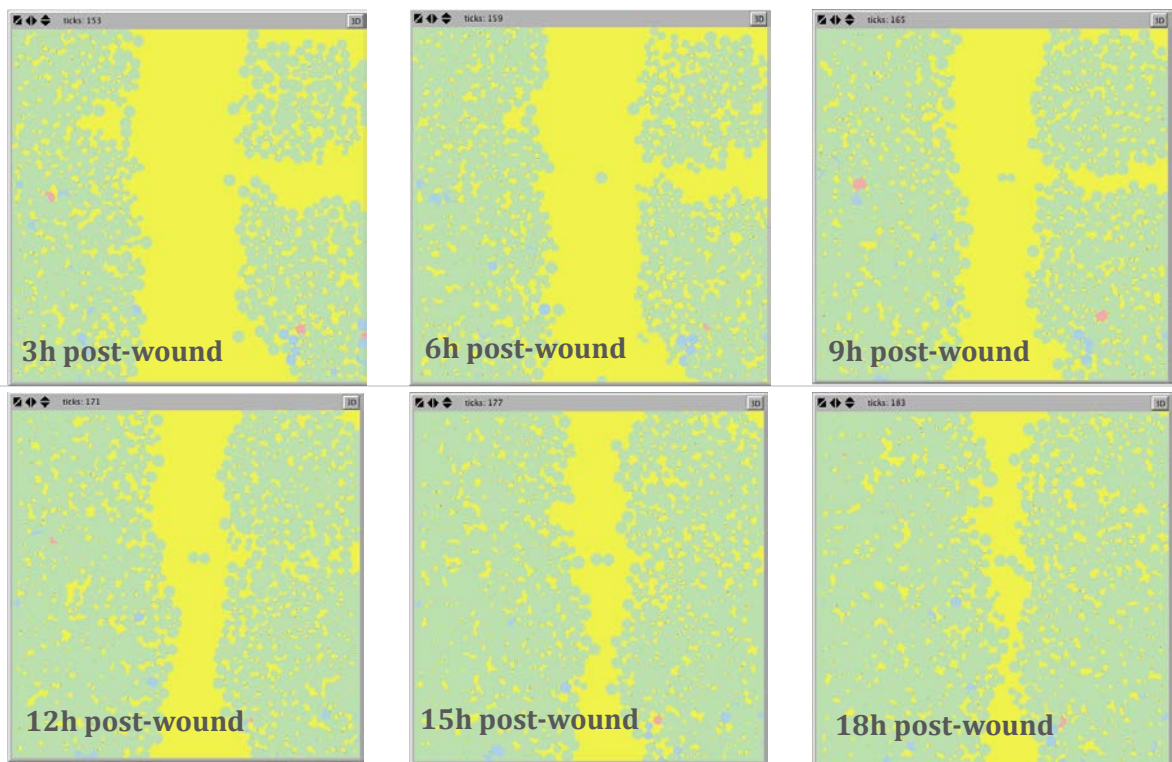


Figure 6. Wound- healing follow-up at three-hour intervals for urothelial cells at high calcium concentrations.

In the case of high calcium concentrations, it was observed that healing was faster than at low calcium concentration, when the wound was caused at full confluence; however, this might be due to the fact that to reach full confluence, a higher number of cells is needed at high calcium conditions. When the wound was caused with a

similar number of cells, wound repairing was actually slower than at low calcium concentrations (Figure 6).

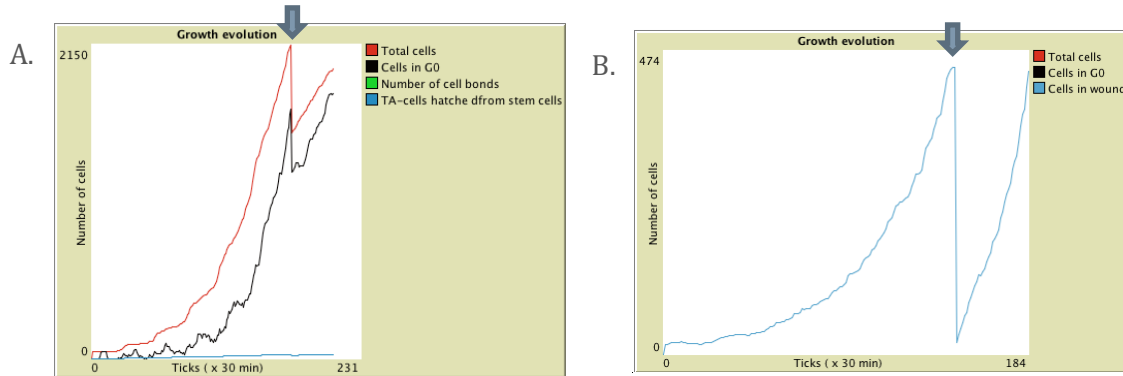


Figure 7. A. Growth evolution of urothelial cells after wound (indicated with arrow). B. Evolution of number of cells occupying the space of the wound. High calcium concentration conditions.

Growth rate results (Figure 7A) show that growth post-wound has a slower rate, and the number of cells after 18 hours does not surpass the number of cells at the moment of wounding. The cells occupying the wound (Figure 7B) seem to equal the number of cells present before the wound was caused; however, taking into account that confluence was not complete and that in this space there might have been gaps prior to the wound, this means that the wound was not fully closed after 18 hours.

These results suggest that cellular migration towards the wound space is important for a rapid tissue healing, and thus that low calcium concentrations yield a faster wound closing than high concentrations, which is coherent with the findings of Walker et al. (2004).

2. Keranocytes

Due to the slow growth rate of keranocytes, and limited computational resources, a full wound closing could not be observed, even by studying long intervals of time. Below, the different wound progressions are shown, as well as the population dynamics of the high calcium concentration condition.

The most remarkable observation of this simulation corresponds to the cell growth post-wounding. In XXX, it is observed that the growth rate of the total number of cells coincides with the growth of the TA-cells that were spawned from stem cells. This means that in this model it is stem cells who are in charge of wound repairing, given that the rest of the cells have reached a quiescent state.

a. Low calcium concentration

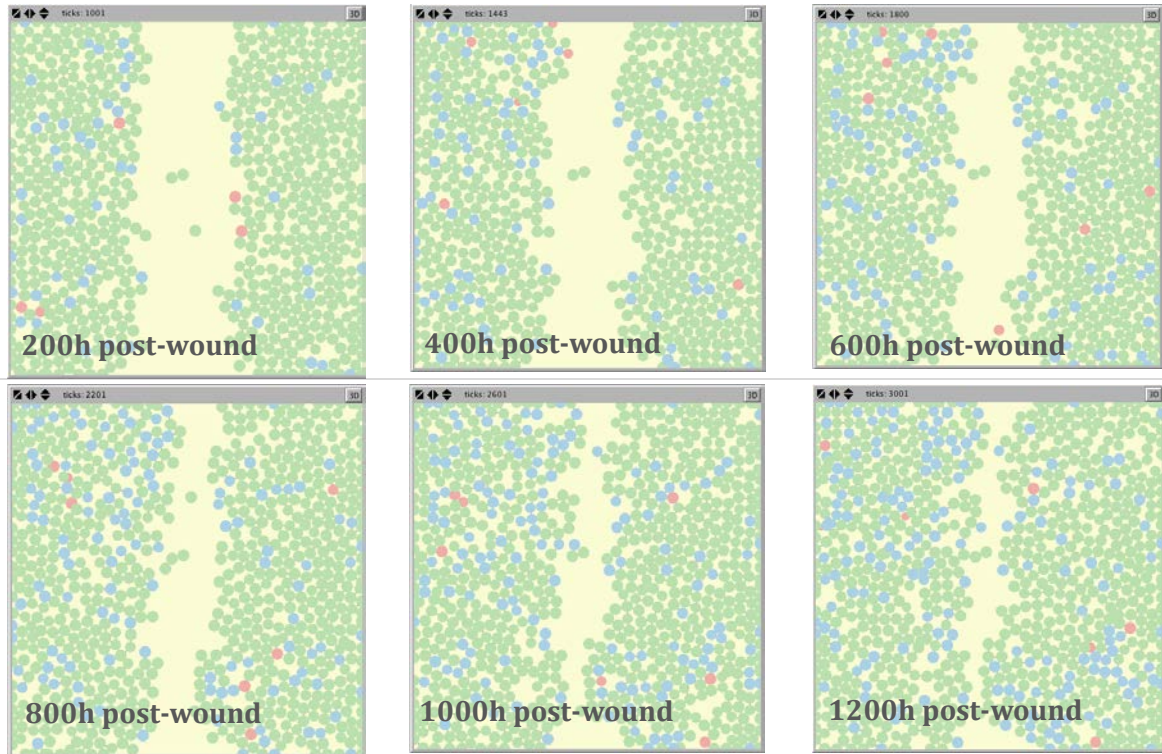


Figure 8. Wound- healing follow-up at 200-hour intervals for keranocytes at low calcium concentrations.

b. High calcium concentration

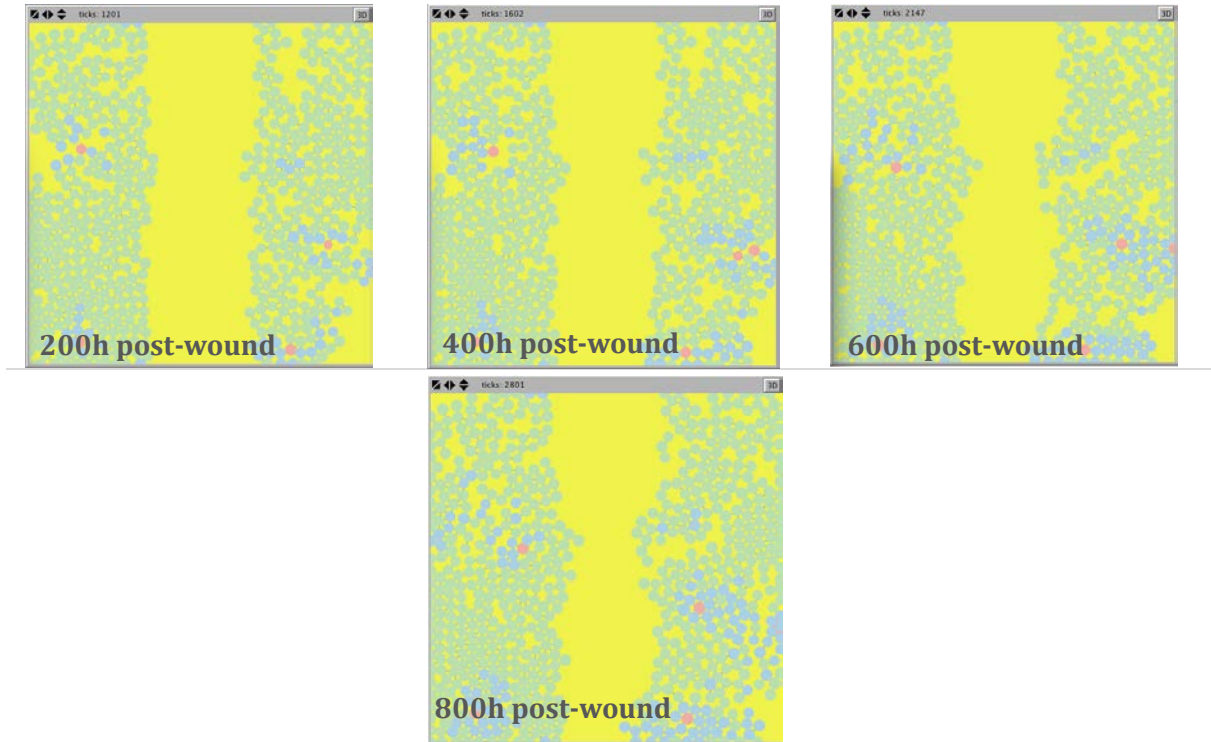


Figure 9. Wound- healing follow-up at 200-hour intervals for keranocytes at high calcium concentrations.

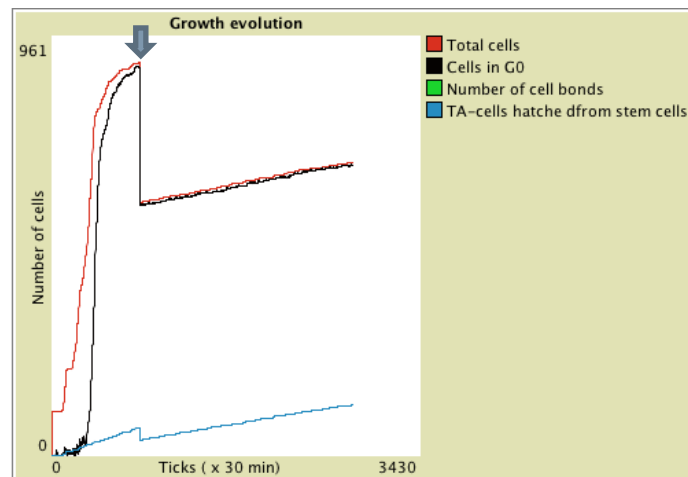


Figure 10. Growth evolution of keranocytes at high calcium concentrations after wound (indicated with arrow).

Conclusions

Despite some drawbacks and limitations, the present model was able to mimic the behaviour of the epithelial cells modelled by the epitheliome of Walker et al. (2004).

It could be observed that cell growth was dependent of the cellular type, namely the maximum number of divisions allowed for each one, as well as the initial number of seeds. Keranocytes showed a slow growth rate compared to urothelial cells, which had virtually no limitations in their number of divisions (for the number of iterations considered in this study).

Extracellular calcium concentration showed an important effect on cell migration and wound healing. High calcium concentrations increased the number of intercellular bonds and thus of migrating cells. This resulted in a differential cellular growth pattern for both calcium concentrations, as well as a significant difference in the time of wound repairing.

It was also observed that when there is a stringent limitation in the number of divisions, stem cells seem to play an important role in population growth and tissue repairing.

Further simulations can be performed in order to study the dynamics of the cell cycle, by for instance gathering data on the number of cells in all cell cycle stages.

References

Walker DC, Southgate J, Hill G, Holcombe M, Hose DR, Wood SM, Mac Neil S, Smallwood RH. The epitheliome: agent-based modelling of the social behaviour of cells. *Biosystems*. 2004 Aug-Oct;76(1-3):89-100

Walker DC, Hill G, Wood SM, Smallwood RH, Southgate J. Agent-based computational modelling of wounded epithelial cell monolayers. *IEEE Trans Nanobioscience*. 2004 Sep;3(3):153-63

Wilensky, U. (1999). NetLogo. <http://ccl.northwestern.edu/netlogo/>. Center for Connected Learning and Computer-Based Modeling, Northwestern University, Evanston, IL.

Baumgartner, W., Hinterdorfer, P., Ness, W., Raab, A., Vestweber, D., Schindler, H., Drenckhahn, D., 2000. Cadherin interaction probed by atomic force microscopy. *Proc. Natl. Acad. Sci. U.S.A.* 97 (8), 4005–4010.